

## Antiglioma action of xanthones from *Gentiana kochiana*: Mechanistic and structure–activity requirements

Aleksandra Isakovic,<sup>a</sup> Teodora Jankovic,<sup>b</sup> Ljubica Harhaji,<sup>c</sup> Sladjana Kostic-Rajacic,<sup>d</sup>  
Zoran Nikolic,<sup>e</sup> Vlatka Vajs<sup>d</sup> and Vladimir Trajkovic<sup>f,\*</sup>

<sup>a</sup>Institute of Biochemistry, School of Medicine, University of Belgrade, Belgrade, Serbia

<sup>b</sup>Institute for Medicinal Plant Research “Dr Josif Pancic”, Belgrade, Serbia

<sup>c</sup>Institute for Biological Research “Sinisa Stankovic”, Belgrade, Serbia

<sup>d</sup>Institute for Chemistry, Technology and Metallurgy, Belgrade, Serbia

<sup>e</sup>Faculty of Physics, University of Belgrade, Belgrade, Serbia

<sup>f</sup>Institute of Microbiology and Immunology, School of Medicine, University of Belgrade, Dr. Subotica 1, 11000 Belgrade, Serbia

Received 15 January 2008; revised 14 March 2008; accepted 25 March 2008

Available online 30 March 2008

**Abstract**—The present study identifies xanthones gentiakoichianin and gentiacaulein as the active principles responsible for the in vitro anti glioma action of ether and methanolic extracts of the plant *Gentiana kochiana*. Gentiakoichianin and gentiacaulein induced cell cycle arrest in G<sub>2</sub>/M and G<sub>0</sub>/G<sub>1</sub> phases, respectively, in both C6 rat glioma and U251 human glioma cell lines. The more efficient antiproliferative action of gentiakoichianin was associated with its ability to induce microtubule stabilization in a cell-free assay. Both the xanthones reduced mitochondrial membrane potential and increased the production of reactive oxygen species in glioma cells, but only the effects of gentiakoichianin were pronounced enough to cause caspase activation and subsequent apoptotic cell death. The assessment of structure–activity relationship in a series of structurally related xanthones from *G. kochiana* and *Gentianella austriaca* revealed dihydroxylation at positions 7, 8 of the xanthonic nucleus as the key structural feature responsible for the ability of gentiakoichianin to induce microtubule-associated G<sub>2</sub>/M cell block and apoptotic cell death in glioma cells.

© 2008 Elsevier Ltd. All rights reserved.

### 1. Introduction

*Gentiana kochiana* Perr. et Song. (*Gentianaceae*) is a widespread South European species, growing at altitudes between 1500 and 3000 m.<sup>1</sup> Like other *Gentiana* species throughout the world, *G. kochiana* has been used in the traditional medicine in the region of Tuscany,<sup>2</sup> and the roots of this plant are employed as antihypertensive, antipyretic, spasmolytic, and bitter-tonic.<sup>3</sup> Xanthone aglycones and glycosides are among the major identified components in *G. kochiana*.<sup>4</sup> Xanthones, including those isolated from *G. kochiana*, display various pharmacological effects, including antioxidant, CNS depressant or stimulant, antidiabetic, antiinflammatory, and antitumor actions.<sup>5</sup> This might explain the growing interest in this class of compounds, demonstrated by the large number of the newly isolated and synthesized derivatives during the last decade.<sup>6</sup> While the anticancer

effect of different plant and synthetic xanthones has been consistently demonstrated in numerous studies,<sup>5,7–13</sup> the xanthones from *G. kochiana* have not been tested for their antitumor activity. Moreover, the molecular mechanisms underlying the observed anticancer effect of xanthones have only been sporadically investigated. Actually, most of the data regarding the mechanisms of xanthone antitumor activity were reported for  $\alpha$ -mangostin, the prenylated xanthone from the *Garcinia mangostana* L., which affects the expression of cell cycle-regulating cyclins and induces mitochondria-dependent apoptosis.<sup>14–16</sup>

Gliomas are extremely aggressive neuroectodermal tumors that represent the most common primary malignancy in human central nervous system.<sup>17</sup> Gliomas are incurable in most of the cases and are notorious for their ability to resist chemotherapy and radiation-induced apoptosis.<sup>17</sup> The aim of the present study was to investigate the in vitro anti glioma activity of different xanthone-containing *G. kochiana* extracts and identify their active principles, as well as their mechanisms of

**Keywords:** Xanthone; Glioma; Cell cycle; Apoptosis; Oxidative stress.

\*Corresponding author. Tel./fax: +381 11 265 7258; e-mail: [vtrajkovic@eunet.yu](mailto:vtrajkovic@eunet.yu)

action. Moreover, using a series of structurally related xanthenes, we sought to acquire some insight into the structure–activity relationship for the observed antiglioma effect.

## 2. Results

### 2.1. Antiglioma action of *G. kochiana* extracts and isolated xanthenes

To initially test the antiglioma activity of xanthone-containing *G. kochiana* extracts and isolated xanthenes, we used crystal violet and MTT assay to measure cell numbers and mitochondrial activity, respectively. The HPLC analysis of the extracts confirmed that the ether extract contained mainly xanthone aglycones **1**, **2**, and **3**, the butanolic extract was rich in xanthone glycosides **4**, **5**, and **6**, while the methanolic extract contained both aglycones and glycosides (Fig. 1A–C). The crystal violet test performed after 48 h cultivation of C6 and U251 glioma cells with plant extracts revealed the following order of growth-inhibiting potency: ether extract (containing mainly aglycones) > methanolic extract (aglycones + glycosides) > butanolic extract (mainly glycosides) (Fig. 2A). Accordingly, xanthone aglycones **1** and **2** displayed significant antiglioma effect, while the corresponding glycosides **4**, **5** and **6** ( $IC_{50} > 100 \mu M$ ) were only marginally active (Fig. 2B and C). Aglycone **1**

( $IC_{50} = 27.3 \pm 3.7 \mu M$  and  $31.4 \pm 8.6 \mu M$  for U251 and C6 cells, respectively;  $n = 3$ ) was more efficient than compound **2** ( $IC_{50} = 53.2 \pm 5.7 \mu M$  and  $56.6 \pm 5.7$  for U251 and C6 cells, respectively;  $n = 3$ ), while aglycone **3** ( $IC_{50} > 100 \mu M$ ) was markedly less active in comparison with either **1** or **2** (Fig. 2B). To obtain additional data for the structure–activity relationship analysis, we also tested the antiproliferative effect of the two xanthenes (**7** and **8**) from *Gentianella austriaca*. Both **7** and **8** ( $IC_{50} > 100 \mu M$ ) displayed the antiglioma effect comparable to that of **3** and were significantly less active than **1** and **2** (Fig. 2D). The antiglioma effect of xanthenes **1** and **2** was evident after 24 h of treatment and persisted for at least 72 h, as confirmed in a time-dependence study using both crystal violet assay and MTT test for mitochondrial activity (Fig. 3). Therefore, xanthone aglycones gentiakochoianin (**1**) and gentiacaulein (**2**) represent active principles responsible for the antiglioma effect of ether and methanolic extracts of *G. kochiana*.

### 2.2. Synergistic and antagonistic interactions of gentiakochoianin, gentiacaulein, and decussatin in inhibiting the glioma cell growth

To get some insight into the mechanisms of xanthone antiglioma effect, we tested the nature (additive, synergistic, or antagonistic) of their interaction upon combined treatment. The analysis based on Chou–Talalay

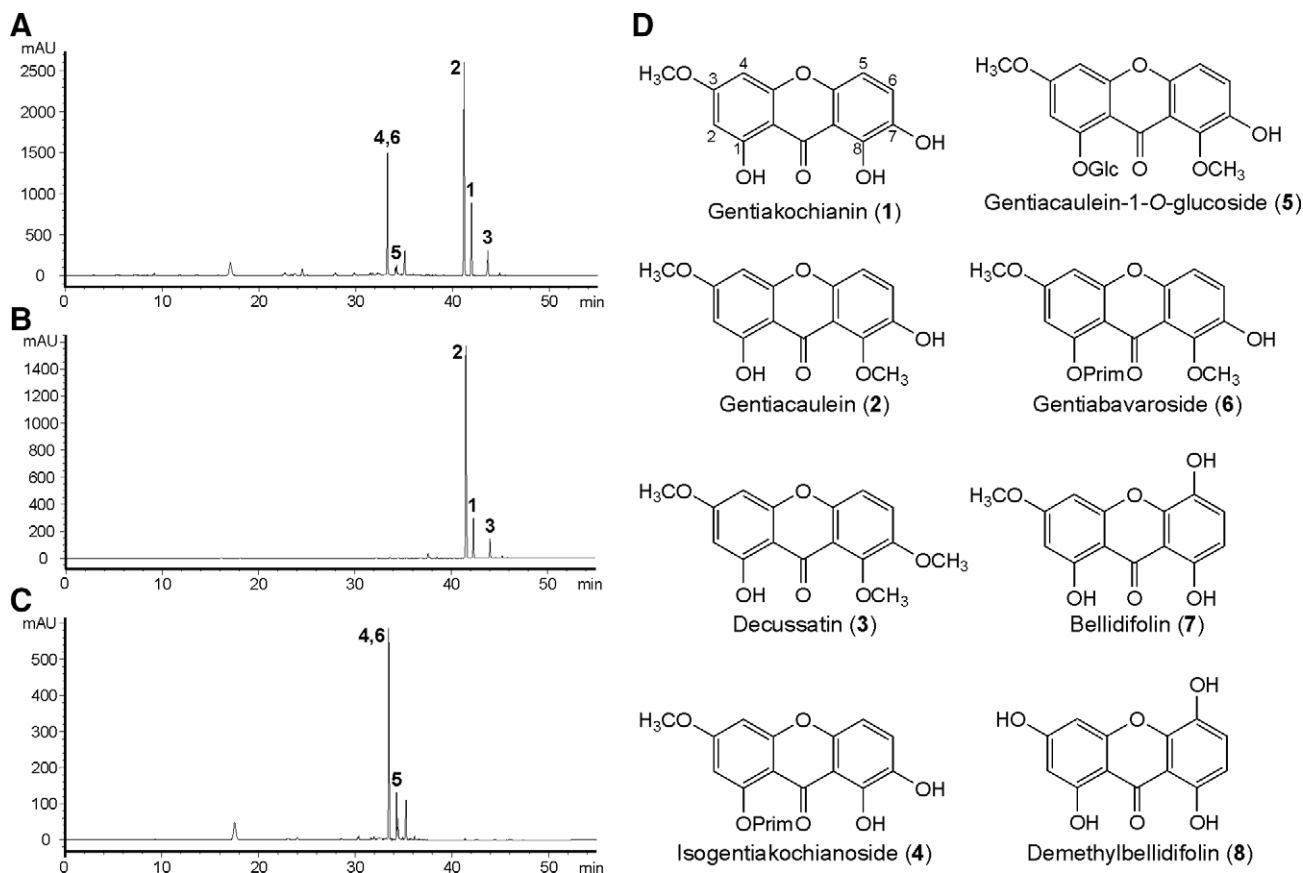


**Figure 1.** (A–C) HPLC analysis of methanolic (A), ether (B), and butanolic (C) extracts of *G. kochiana*. (D) Chemical structure of xanthenes from *G. kochiana* (**1–6**) and *G. austriaca* (**7** and **8**).

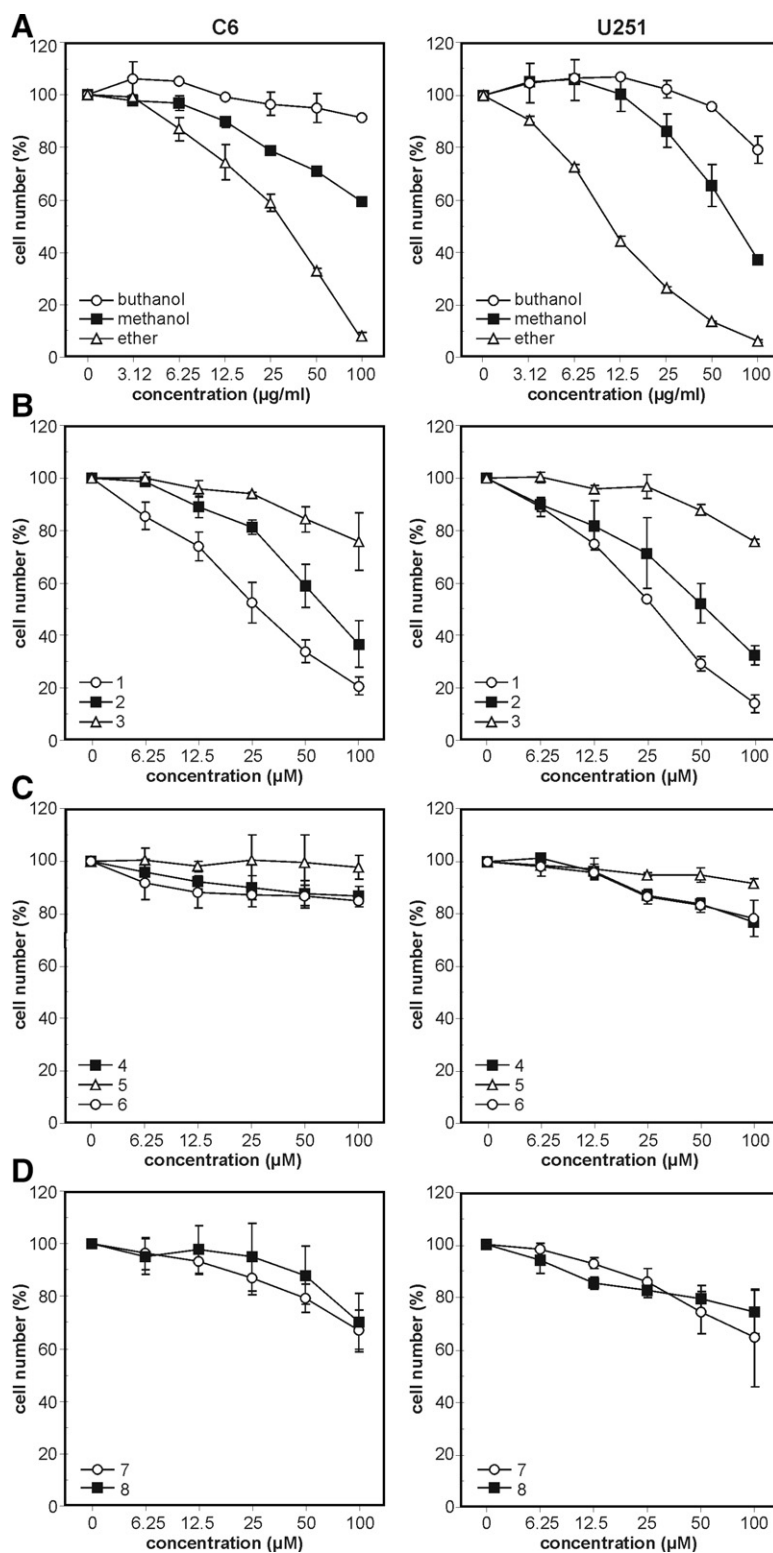


**Figure 2.** Antiglioma action of xanthone-containing plant extracts and isolated xanthones. C6 (left) and U251 glioma cells (right) were incubated with different concentrations of plant extracts (A) or isolated xanthones **1**, **2**, **3** (B), **4**, **5**, **6** (C) **7** or **8** (D). The cell number was assessed after 48 h by crystal violet staining. The results are presented as means  $\pm$  SD values of triplicate observations from a representative of three experiments (A) or as mean  $\pm$  SD values from four (B) or three (C and D) independent experiments.

median-effect principle revealed that the combinations of gentiacaulein (**2**) with either gentiakochianin (**1**) or decussatin (**3**) displayed a synergistic interaction (combination index  $< 1$ ) throughout 0.1–0.99 efficiency range

(Fig. 4). On the other hand, **1** and **3** showed a synergistic interaction only at higher cytotoxic efficiencies, while the antagonism (combination index  $> 1$ ) was clearly evident at the lower efficiency levels (Fig. 4). Similar results were

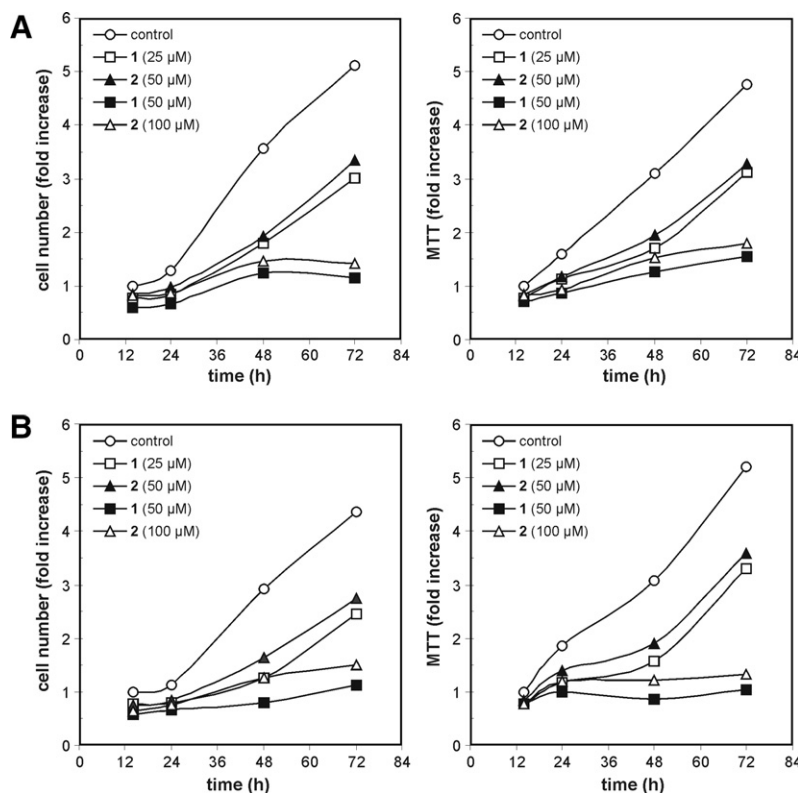


**Figure 3.** Time-dependence of xanthone antiglioma effect. (A) C6 and (B) U251 glioma cells were incubated with xanthones **1** or **2** and the cell number (crystal violet) and mitochondrial dehydrogenase activity (MTT) were assessed at the indicated time points. The results are presented as mean values of triplicate observations from one of two experiments with similar results (SD values were within 10% of the mean values).

also obtained with U251 cells (not shown). Therefore, the absence of additive interactions indicates that the tested xanthones might employ different mechanisms for their antiglioma effects.

### 2.3. Distinct effects of gentiakoichianin and gentiacaulein on cell cycle progression and microtubule depolymerization in glioma cells

In order to further explore the observed antiglioma effects of gentiakoichianin (**1**) and gentiacaulein (**2**), we tested their ability to influence the cell cycle progression. In accordance with the Chou–Talalay analysis, indicating that different mechanisms might mediate antiglioma action of **1** and **2**, the propidium iodide-based analysis of the DNA content in C6 glioma cells revealed a distinct pattern of cell cycle modulation by the two xanthones. While treatment with **1** led to a significant accumulation of cells in  $G_2/M$  phase of the cell cycle, compound **2** caused a cell cycle arrest in  $G_0/G_1$  phase (Fig. 5A). Since the interference with microtubule dynamics is one of the mechanisms for the blockade of cell division, we have measured the ability of various xanthones to affect microtubule depolymerization. While gentiakoichianin (**1**) inhibited microtubule disassembly with the  $IC_{50}$  value of 18 μM, gentiacaulein (**2**), as well as compounds **7** and **8** were inactive in the microtubule depolymerization assay ( $IC_{50} > 50$  μM) (Fig. 5B). The  $IC_{50}$  for the well-known microtubule-stabilizing drug taxol was 2.4 μM (Fig. 7). Decussatin (**3**) was not tested due to a limited compound availability. There-

fore, among the xanthones tested, only gentiakoichianin (**1**) exerted a significant microtubule-stabilizing effect, which is consistent with its ability to block cell cycle progression in the  $G_2/M$  phase.

### 2.4. Distinct effects of gentiakoichianin and gentiacaulein on the induction of apoptosis in glioma cells

In addition to the suppression of cell proliferation, the observed antiglioma activity of the investigated xanthones could also result from the induction of cell death. Therefore, we next assessed the ability of gentiakoichianin (**1**) and gentiacaulein (**2**) to induce apoptotic or necrotic cell death in glioma cell cultures. The microscopical examination revealed that xanthone-treated glioma cultures contained less cells than control, untreated cultures (Fig. 6A). However, while compound **2** did not significantly affect the morphology of glioma cells, many cells in compound **1**-treated cultures lost their normal polygonal shape and became round (Fig. 6A). This was consistent with the induction of glioma cell death upon exposure to compound **1**, which was confirmed by an increase in numbers of apoptotic cells ( $Ann^{+}PI^{-}$  cells) displaying the apoptotic marker phosphatidylserine on the intact cell membranes (Fig. 6B). On the other hand, we failed to observe a significant increase in the numbers of either apoptotic ( $Ann^{+}PI^{-}$ ) or necrotic ( $Ann^{+}PI^{+}$ ) cells in glioma cell cultures exposed to compound **2** (Fig. 6B). Accordingly, apoptosis induced by compound **1** was associated with the activation of apoptosis-executing enzymes belonging

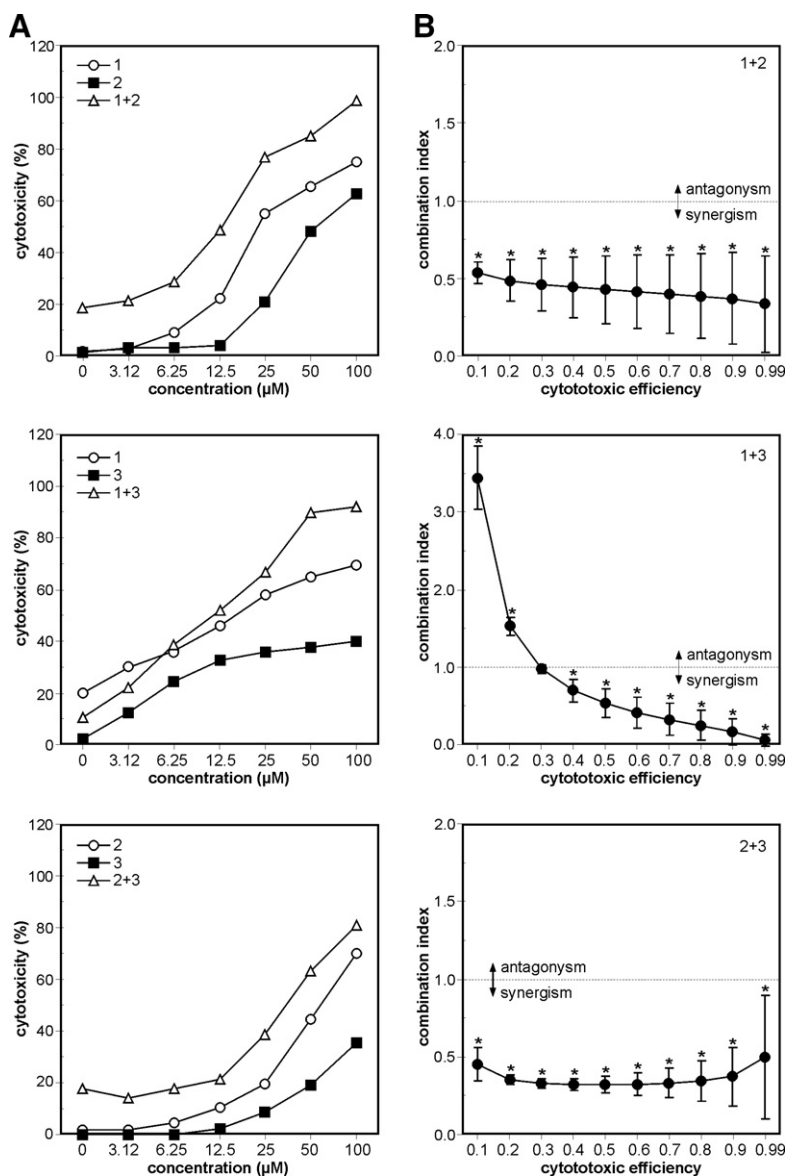


**Figure 4.** Xanthone interactions in reducing glioma growth. (A) C6 cells were incubated with the indicated concentrations of 1, 2 or 3 alone, as well as with their appropriate combinations and the cytotoxicity was assessed after 48 h by crystal violet assay. (B) The values of combination index, reflecting synergistic (<1), antagonistic (>1), or additive interactions (=1) were calculated according to Chou–Talalay median-effect principle. The data are mean values of triplicates from a representative of three experiments (SD < 10% of corresponding mean values) (A) or mean  $\pm$  SD values from three separate experiments (\* $p$  < 0.05 denotes values significantly different from 1).

to caspase family, while compound **2** was unable to cause caspase activation in C6 glioma cells (Fig. 6C). Therefore, a  $G_2/M$  cell cycle block induced by compound **1** was coupled with the induction of apoptotic cell death, while the antiglioma activity of compound **2** was limited to the proliferation arrest in  $G_0/G_1$  cell cycle phase. Results similar to those presented in Fig. 6 were also obtained with U251 cells (data not shown).

## 2.5. The effects of gentiokochianin and gentiacaulein on mitochondrial membrane potential and oxidative stress induction in glioma cells

The induction of apoptosis is frequently associated with oxidative stress-dependent mitochondrial dysfunction, which is one of the crucial events leading to caspase

activation.<sup>18</sup> Thus, we next examined the ability of gentiokochianin (**1**) and gentiacaulein (**2**) to affect mitochondrial membrane potential and reactive oxygen species (ROS) production in glioma cells. Both the xanthones were able to trigger mitochondrial depolarization in C6 cells, as confirmed by an increase in green-to-red fluorescence ratio (FL1/FL2) of the mitochondria-binding dye DePsipher (Fig. 7A and B). In accordance with its pro-apoptotic activity, compound **1** was markedly more efficient in reducing the mitochondrial membrane potential (Fig. 7B). The staining with the redox-sensitive dye DHR demonstrated that both the xanthones were also able to induce ROS generation in C6 glioma cells (Fig. 7C and D). Again, compound **1** was more clearly more efficient than **2** in increasing intracellular ROS production (Fig. 7D). Treatment with



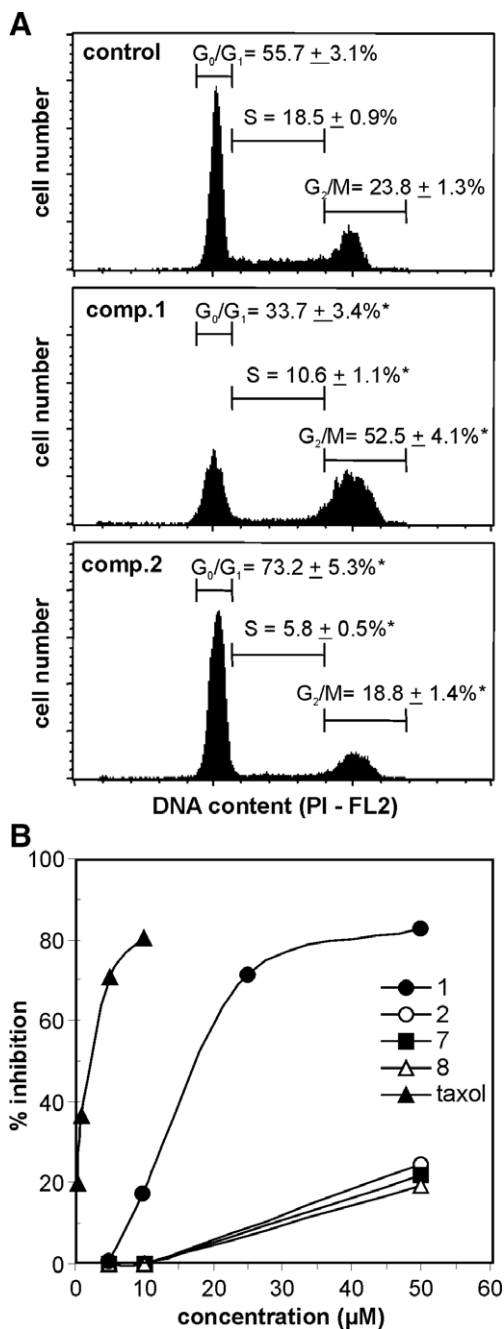


**Figure 5.** Distinct effects of **1** and **2** on cell cycle progression and microtubule depolymerization in glioma cells. (A) C6 cells were incubated with  $50 \mu\text{M}$  of compound **1** or **2**, and the cell cycle was investigated after 24 h by flow cytometry. The representative histograms are presented, while the cell numbers (%) in each graph represent means  $\pm$  SD values from at least three-independent experiments (\* $p < 0.05$  denotes significant difference in comparison with control). (B) Different concentrations of xanthones **1**, **2**, **7**, and **8** were tested for the ability to inhibit microtubule depolymerization in a cell-free system (microtubule-stabilizing drug taxol was used as a positive control). Results are presented as % inhibition of microtubule disassembly (similar results were obtained in another experiment).

the antioxidant agent *N*-acetylcysteine led to a partial recovery of C6 glioma cells exposed to compound **1** (Fig. 7E), which was associated with the reduction of caspase activation (Fig. 7F). On the other hand, such a protective effect of *N*-acetylcysteine could not be

observed in cell cultures exposed to compound **2** (Fig. 7E). Results similar to those presented in Figure 7 were also obtained with U251 cells (not shown). Therefore, the ability of compound **1** to trigger apoptotic death of glioma cells was associated with the induction of mitochondrial depolarization and oxidative stress.

## 2.6. The effects of gentiakoichianin and gentiacaulein on the viability of primary astrocytes and macrophages

To examine if the primary, non-transformed cells are also susceptible to antiproliferative/cytotoxic effect of gentiakoichianin (**1**) and gentiacaulein (**2**), the cultures of rat primary astrocytes were exposed to xanthones for 48 h. Both crystal violet and MTT assays revealed that rat astrocytes were significantly more resistant to xanthone-induced growth inhibition ( $\text{IC}_{50} > 100 \mu\text{M}$ ; Fig. 8A) in comparison with their transformed counterparts. Accordingly, neither **1** nor **2** was able to cause changes in astrocyte morphology that would be visible under inverted bright-field microscope (Fig. 8B). Moreover, the numbers (crystal violet) and mitochondrial respiration (MTT) of rat peritoneal macrophages were not at all affected by exposure to either **1** or **2** ( $\text{IC}_{50} > 100 \mu\text{M}$ ) (Fig. 8C), thus confirming that their antiproliferative/cytotoxic effects were fairly selective for the transformed glial cells.

## 3. Discussion

The present study for the first time describes gentiakoichianin (**1**) and gentiacaulein (**2**) as the active principles responsible for the in vitro anti-glioma effect of xanthone-containing *G. kochiana* extracts. However, the mechanisms underlying the observed effects of the two xanthones were profoundly different. While gentiakoichianin-induced microtubule stabilization-associated  $G_2/M$  cell cycle block, treatment with gentiacaulein led to a  $G_0/G_1$  cell cycle arrest (Fig. 9). Moreover, both the xanthones were able to induce oxidative stress and mitochondrial depolarization in glioma cells, but the effects of compound **1** were more pronounced and resulted in the induction of caspase activation and subsequent apoptotic cell death (Fig. 9). Importantly, the primary astrocytes and macrophages were markedly more resistant than glioma cells to the antiproliferative/cytotoxic action of compounds **1** and **2**.

The property of microtubules, termed dynamic instability, to undergo rapid cycles of polymerization and depolymerization, is essential for various cellular functions, including the cell cycle progression.<sup>19</sup> Several anticancer drugs with proven clinical utility act by disrupting microtubule dynamics, including microtubule destabilizing drugs such as vinblastine and the stabilizing drug taxol.<sup>20</sup> While the ability to disrupt microtubule dynamics has recently been demonstrated for some flavones,<sup>21</sup> the present study for the first time demonstrates that xanthone gentiakoichianin can stabilize microtubules and prevent their depolymerization with the efficiency that is less than one order of magnitude lower when

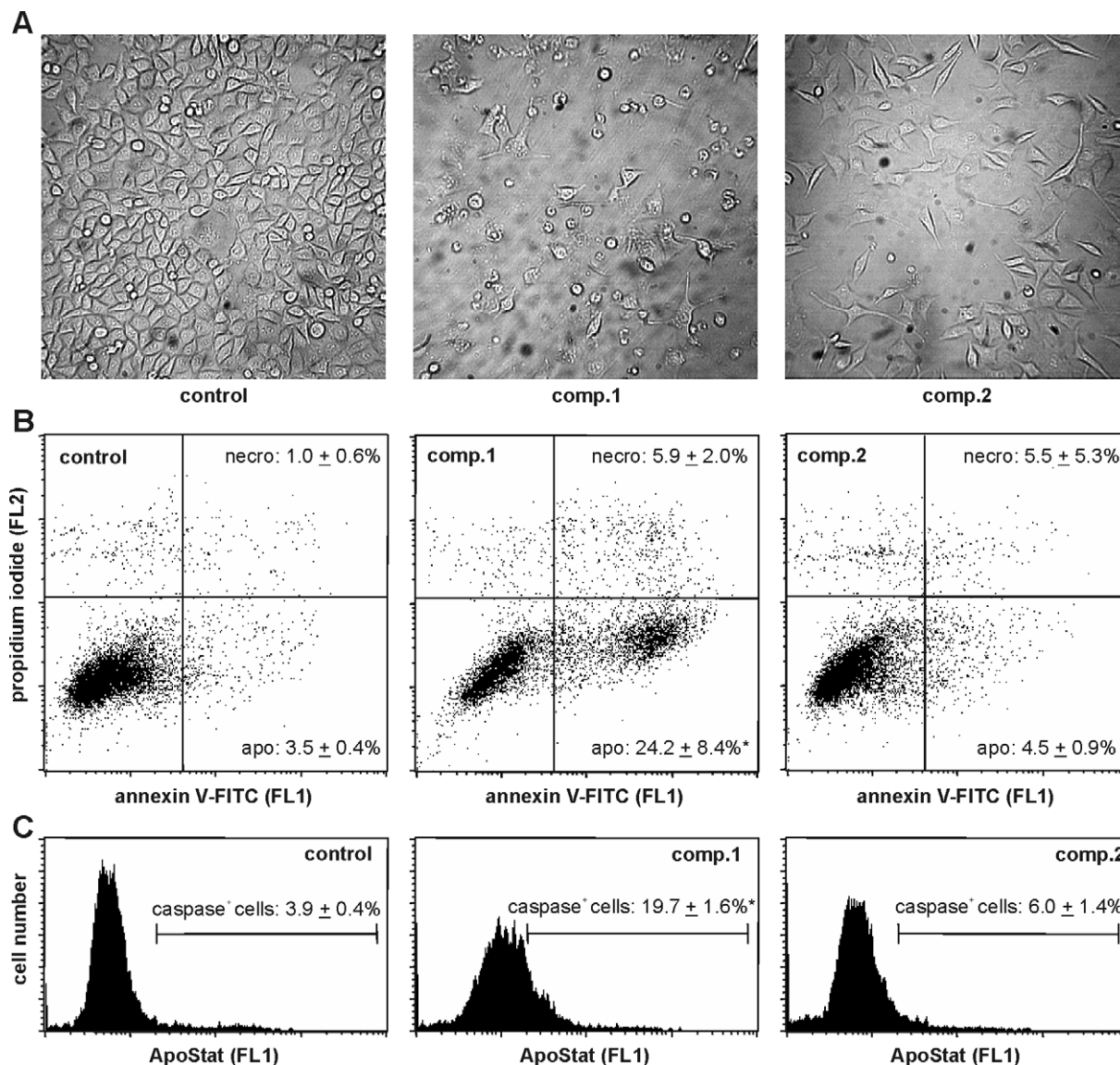


**Figure 6.** Distinct effects of **1** and **2** on the induction of apoptosis in glioma cells. C6 cells were incubated with 50  $\mu$ M of compound **1** or **2** and the cell morphology (A; 48 h), the induction of apoptosis/necrosis (B; 36 h) or caspase activation (C; 36 h) was investigated by inverted bright-field microscopy (A) or flow cytometry (B and C). The representative dot blots or histograms (B and C) are presented, while the cell numbers (%) in each graph represent means  $\pm$  SD values from at least three-independent experiments (\* $p < 0.05$  denotes significant difference in comparison with control).

compared with that of taxol. This is consistent with the ability of gentiakoichianin to efficiently block cell cycle progression in  $G_2/M$  phase, which is also a hallmark of the taxol's anticancer action.<sup>22</sup> It should be noted, however, that the cytotoxic activity of gentiakoichianin observed in the present study was several orders of magnitude lower than that of taxol,<sup>22</sup> in spite of the fairly comparable microtubule-stabilizing efficiencies. This discrepancy could be at least partly explained by the fact that we used an in vitro cell-free assay for tubulin depolymerization, and it has been known that tubulin dynamics in vivo might significantly differ from that in vitro.<sup>19</sup>

Microtubule stabilization by taxol and subsequent  $G_2/M$  cell cycle block are associated with caspase-dependent induction of apoptosis in cancer cells.<sup>23,24</sup> This is consistent with the ability of compound **1** to induce caspase

activation and apoptotic death of glioma cells in our study. These effects were partly blocked with the well-known antioxidant agent *N*-acetylcysteine, suggesting a role for the oxidative stress in compound **1**-triggered apoptosis of glioma cells. The excessive production of ROS could trigger the opening of mitochondrial permeability transition pore, which is associated with mitochondrial depolarization and subsequent release of small molecules such as cytochrome *c*, that cause activation of caspase cascades.<sup>18</sup> Moreover, the collapse of the mitochondrial membrane potential triggers an increase in ROS generation by the electron transfer chain, which provides a positive feedback mechanism for enhanced ROS production leading to further mitochondrial and cellular injury.<sup>25</sup> As compound **1** was able to induce mitochondrial depolarization in glioma cells, it is conceivable to assume that similar scenario was functional in compound **1**-triggered caspase activation and

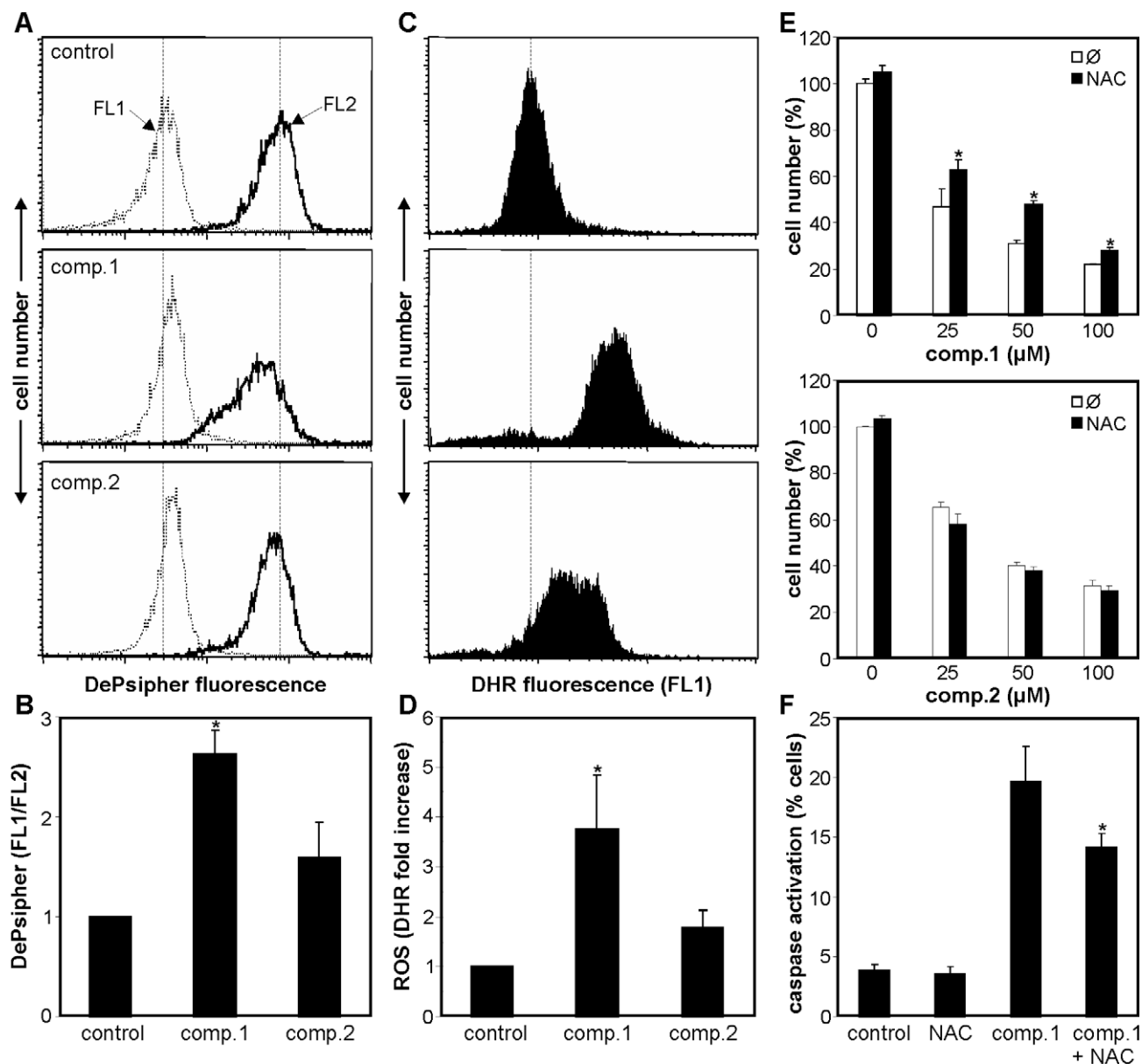


**Figure 7.** The effects of **1** and **2** on the induction of ROS and mitochondrial depolarization in glioma cells. (A–D) C6 cells were incubated with 50 μM of compound **1** or **2**, and mitochondrial membrane potential (A; 24 h) or ROS production (C; 36 h) was investigated by flow cytometry. The results from representative histograms are presented (vertical line represents the mean fluorescence value of the control sample). The values of FL1/FL2 mean fluorescence ratio (B) and mean fluorescence intensity (D), reflecting mitochondrial depolarization and ROS production, respectively, are mean ± SD values from three different experiments (\* $p < 0.05$  refers to both control and compound **2** treatment). (E) C6 cells were incubated for 48 h with different concentrations of **1** or **2**, in the presence or absence of *N*-acetylcysteine (NAC; 2 mM), and the cell number (mean ± SD from three experiments; \* $p < 0.05$  refers to corresponding treatment without NAC) was assessed by crystal violet staining. (F) Caspase activation (mean ± SD from three experiments; \* $p < 0.05$  refers to treatment with compound **1** alone) in C6 cells exposed to compound **1** and/or *N*-acetylcysteine was determined after 36 h by flow cytometry.

apoptosis. However, since xanthenes possess mainly antioxidant properties, it does not seem likely that compound **1** itself was a source of ROS. A more plausible situation is that ROS were generated by mitochondria following the interaction with compound **1** and subsequent loss of mitochondrial membrane potential. This is consistent with the fact that taxol acts directly on isolated mitochondria to release cytochrome *c*,<sup>26</sup> presumably through interaction with mitochondrial tubulin that could play a role in apoptosis via interaction with

the permeability transition pore.<sup>27</sup> On the other hand, xanthenes that induce  $G_0/G_1$  cell cycle block, such as  $\alpha$ -mangostin<sup>15</sup> and compound **2**, share the ability of compound **1** to cause mitochondrial depolarization, suggesting that compound **1** could also exert its effects on mitochondria independently of tubulin stabilization. The apparent structural similarity between xanthone derivatives and mitochondria-binding dye dihydrorhodamine 123<sup>28</sup> supports such an assumption. Accordingly, it has been demonstrated that mangiferin, a naturally



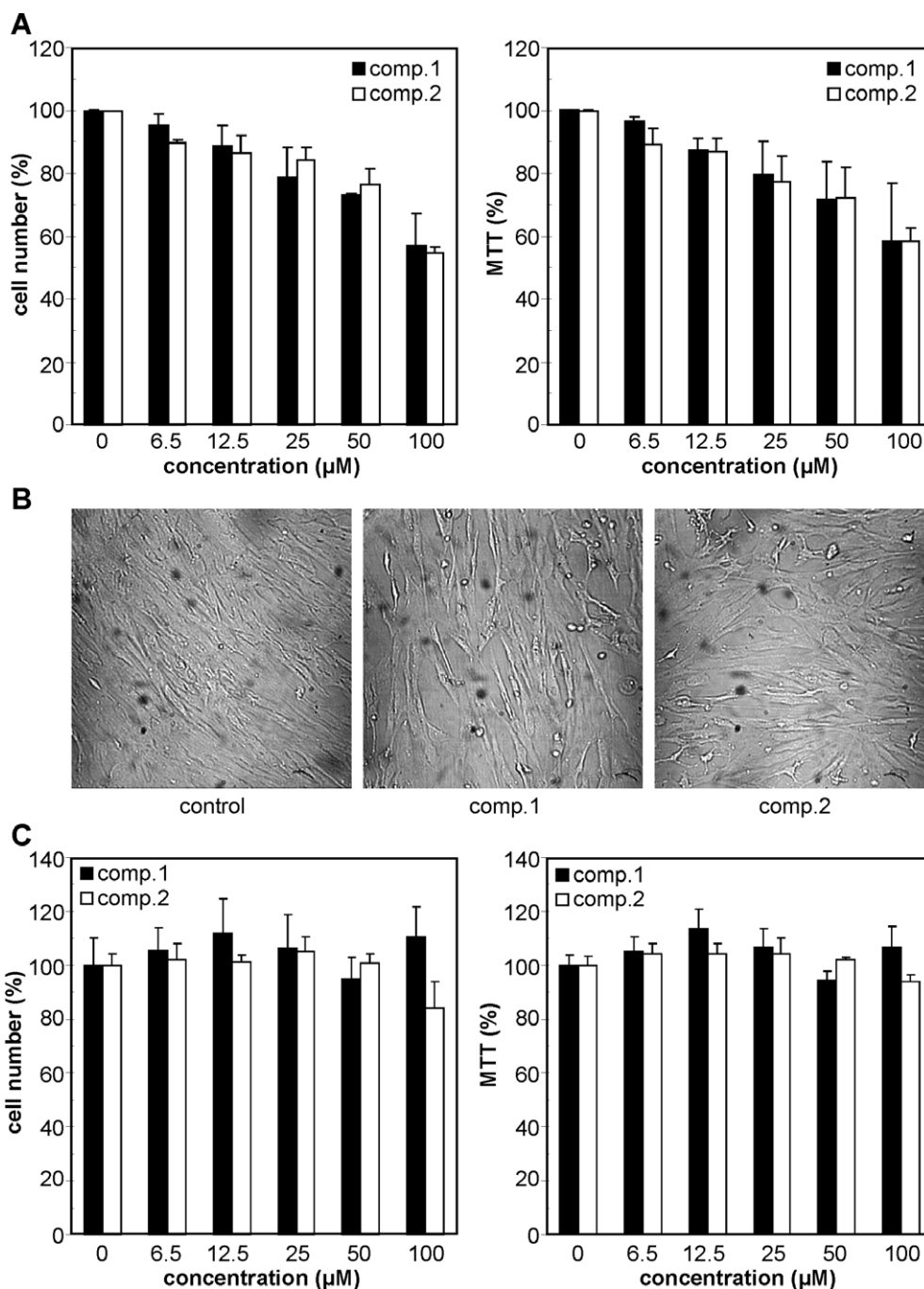


**Figure 8.** The effects of **1** and **2** on rat primary astrocytes and macrophages. (A and B) Rat primary astrocytes were exposed for 48 h to different doses of **1** or **2**. The cell numbers or mitochondrial respiration was measured by crystal violet or MTT assay, respectively, while the astrocyte morphology was examined by inverted bright-field microscopy. (C) Rat peritoneal macrophages were incubated with different concentrations of **1** or **2** and the crystal violet or MTT assay was performed after 48 h. (A and C) The results are means  $\pm$  SD values from three-independent experiments (A) or from triplicate observations obtained in one of two experiments with similar results (C).

occurring xanthone, can induce permeability transition in isolated rat liver mitochondria.<sup>29,30</sup> However, the exact mechanisms of xanthone-induced mitochondrial dysfunction are still to be revealed.

The importance of hydroxylation of xanthonic nucleus in acquiring growth inhibitory activity was previously established by findings that parental non-derivatized xanthone as well as monohydroxy derivatives were inac-

tive, while dihydroxylation at various positions of xanthonic nucleus led to a strong increase in antiproliferative capacity.<sup>12</sup> Interestingly, dihydroxyxanthenes with juxtaposed OH groups (1–2, 2–3, 3–4) were more active than their counterparts with non-adjacent OH moieties (1–3, 3–5),<sup>12</sup> which might explain the low activity of 1,3,5-trihydroxy-3-methoxy (compound **7**) and 1,3,5,8-tetrahydroxy (compound **8**) derivatives in our study. Therefore, the juxtaposition of OH groups at

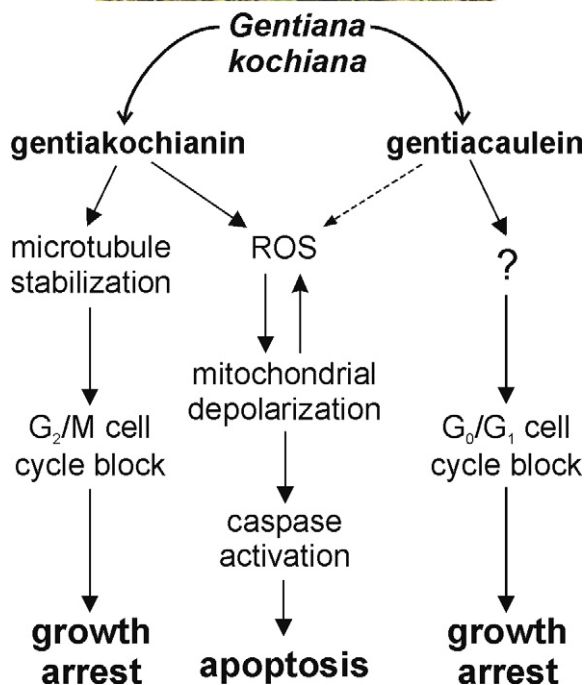


**Figure 9.** Mechanisms underlying the antiglioma action of xanthenes from *G. kochiana* (on the photograph). The ROS induction by gentiacaulein (dashed line) is too weak to induce mitochondrial dysfunction and apoptosis.

positions 7 and 8 might be accountable for the highest activity of compound **1**, which correlated with its ability to induce apoptosis. Accordingly, the substitution of the OH group at position 8 with a methoxy moiety, as the only structural difference between compounds **1** and **2**, was associated with the loss of the pro-apoptotic capacity and decrease in antiglioma activity of the latter. This is consistent with the results showing that 3,4-dihydroxy xanthone is toxic toward various cell types, but that methoxylation at position 4 leads to a complete loss of the activity.<sup>12</sup> Similarly, the anticancer activity of the prenylated xanthone  $\gamma$ -mangostin with juxtaposed OH groups at positions 6 and 7 was markedly higher than that of  $\alpha$ -mangostin, which has methoxy instead of a hydroxy group at position 6.<sup>14</sup> The fact that dimethoxylation at 7, 8 in compound **3** led to a further decrease in the activity in our study is consistent with the fact that dimethoxy xanthenes, in contrast with their dihydroxy counterparts, are completely devoid of antiproliferative capacity.<sup>12</sup> A mechanistic explanation for the observed correlation might lie in the fact that the replacement of hydroxy groups with methoxy groups remarkably reduced the potency of polyhydroxylated xanthenes to decrease the mitochondrial membrane potential.<sup>15</sup> Inter-

estingly, the methoxylation at position 8 in compound **2** in our study did not only led to a loss of pro-apoptotic capacity, but also caused a shift in xanthone ability to affect microtubule dynamics and cell cycle progression—instead of a microtubule stabilization-related  $G_2/M$  block observed with compound **1**, the antiproliferative action of **2** was associated with  $G_0/G_1$  cell cycle arrest and the loss of microtubule-stabilizing activity. However, it still remains to be revealed what mechanisms are responsible for translating these subtle modifications in xanthone structure into such dramatic changes in their ability to influence microtubule dynamics and cell cycle progression. Our finding that glycosylation at position 1 completely inactivated compounds **1** and **2** also deserves further exploration.

#### 4. Conclusion

In conclusion, the present study for the first time describes the antiglioma action of the two xanthenes from *G. kochiana*, providing some insights into the mechanisms and structure–activity relationship of the observed effects. The relative selectivity of xanthone antiproliferative/cytotoxic action toward transformed glial cells makes them worthy of further investigation as potential candidates for glioma therapy. Particularly interesting in that respect is compound **1**, gentiakochoianin, which displayed a very efficient dual antiglioma effect involving both tubulin stabilization-mediated  $G_2/M$  cell cycle arrest and mitochondria-dependent apoptotic cell death.

#### 5. Experimental

##### 5.1. Plant material

Plant material (*G. kochiana*) was collected at mountain Komovi in Montenegro (at ca. 2000 m) during the time of flowering. Air-dried aerial parts were extracted with MeOH for 48 h at room temperature. The extract was evaporated in vacuo to yield brown residue, which was suspended in water and re-extracted with solvents of increasing polarity: Et<sub>2</sub>O, ethyl acetate, and *n*-butanol. The LC-DAD analysis of the methanolic extract indicated the presence of the xanthone aglycones and glycosides, along with secoiridoid swertiamarin. The ether extract was subjected to dry column flash chromatography on silica gel using toluene with increasing amounts of ethyl acetate (10–100%) to give 30 fractions. Fractions 5 and 12 were chromatographed on Sephadex LH-20, eluting with CH<sub>2</sub>Cl<sub>2</sub>/MeOH (1:1), to yield gentiakochoianin (**1**), gentiacaulein (**2**),<sup>4</sup> and decussatin (**3**).<sup>31</sup> Butanolic extract was subjected to CC on polyamide SC<sub>6</sub> using water with increasing amounts of MeOH (0–90%), and xanthone glycosides isogentiakochoianoside (**4**),<sup>31</sup> gentiacaulein-1-*O*-glucoside (**5**),<sup>32</sup> and gentiavaroside (**6**)<sup>31</sup> were isolated. Compounds bellidifolin (**7**) and demethylbellidifolin (**8**)<sup>33</sup> were isolated from *G. austriaca* (*Gentianaceae*) according to the previously published procedure.<sup>34</sup> The plant extracts and xanthenes were dissolved in dimethyl sulfoxide (DMSO) at 10 mg/ml and 50 mM, respectively.

## 5.2. Cell culture

All chemicals were from Sigma (St. Louis, MO) unless specifically stated. The rat glioma cell line C6 and the human glioma cell line U251 were kindly donated by Dr. Pedro Tranque (Universidad de Castilla-La Mancha, Albacete, Spain). Primary astrocytes were isolated from the brains of newborn Albino Oxford rats, while primary macrophages were obtained from peritoneal cavity of Albino Oxford rats as previously described.<sup>35</sup> The cells were incubated at 37 °C in a humidified atmosphere with 5% CO<sub>2</sub>, in a Hepes (20 mM)-buffered RPMI 1640 cell culture medium supplemented with 5% fetal calf serum, 2 mM L-glutamine, 10 mM sodium pyruvate, and penicillin/streptomycin. For the measurement of cell viability or flow cytometric analysis, glioma cells were incubated in 96-well flat-bottom plates (1 × 10<sup>4</sup> cells per well) or 24-well flat-bottom plates (1 × 10<sup>5</sup> cells/well), respectively. Astrocytes and macrophages were seeded in 96-well flat-bottom plates (3 × 10<sup>4</sup> cells/well). After being rested for 24 h, cells were treated with plant extracts or xanthenes as described in Section 2 and figure legends. Control cultures were exposed to the corresponding amount of vehicle (DMSO). However, we observed no influence of DMSO on any of the parameters tested (data not shown).

## 5.3. Determination of cell number and mitochondrial dehydrogenase activity

The number of adherent, viable cells was assessed using a crystal violet assay, while mitochondrial dehydrogenase activity, as another indicator of cell viability, was determined by mitochondria-dependent reduction of 3-(4,5-dimethylthiazol-2-yl)-2,5-diphenyltetrazolium bromide (MTT) to formazan.<sup>36</sup> For the crystal violet staining, at the end of incubation cells were washed with PBS to remove non-adherent cells, and adherent cells were then fixed with methanol and stained with 1% crystal violet solution at room temperature for 10 min. Plates were washed and crystal violet dye was dissolved in 33% acetic acid. The absorbance of the dissolved dye, corresponding to the number of adherent (viable) cells, was measured in an automated microplate reader at 570 nm. In the MTT assay, MTT solution was added to cell cultures in a final concentration of 0.5 mg/ml and the cells were incubated for an additional 1 h. Thereafter, the solution was removed and the cells were lysed in dimethyl sulfoxide. The conversion of MTT to formazan by metabolically viable cells was monitored by an automated microplate reader at 570 nm. The values obtained in both the assays were presented as % of the control, or as fold increase in comparison to the control value that was arbitrarily set to 1.

## 5.4. Cell cycle and apoptosis analysis

The cell cycle was analyzed by measuring the amount of propidium iodide (PI)-labeled DNA in ethanol-fixed cells, exactly as previously described.<sup>37</sup> Apoptotic and necrotic cell death were analyzed by double staining with fluorescein isothiocyanate (FITC)-conjugated annexin V and PI, in which annexin V bound to the apoptotic cells with

exposed phosphatidylserine, while PI labeled the necrotic cells with membrane damage. Staining was performed according to the manufacturer's instructions (BD Pharmingen, San Diego, CA). The green (FL1) and red (FL2) fluorescence of annexin/PI-stained live cells and PI-stained fixed cells was analyzed with FACSCalibur flow cytometer (BD, Heidelberg, Germany), using a peak fluorescence gate to exclude cell aggregates during cell cycle analysis. The numbers of viable (annexin<sup>-</sup>/PI<sup>-</sup>), apoptotic (annexin<sup>+</sup>/PI<sup>-</sup>), and necrotic (annexin<sup>+</sup>/PI<sup>+</sup>) cells, as well as the proportion of cells in different cell cycle phases, were determined with a Cell Quest Pro software (BD). Ten thousand cells (gated to exclude cell debris) have been analyzed in each sample.

## 5.5. Caspase activation

Activation of caspases was measured by flow cytometry after labeling the cells with a cell-permeable, FITC-conjugated pan-caspase inhibitor (ApoStat; R&D Systems, Minneapolis, MN) according to the manufacturer's instructions. The increase in green fluorescence (FL1) is a measure of caspase activity within the individual cells of the treated population. The results are expressed as % of cells containing active caspases.

## 5.6. ROS measurement

Intracellular production of ROS was determined by measuring the intensity of green fluorescence emitted by redox-sensitive dye dihydrorhodamine 123 (DHR; Invitrogen, Paisley, UK), which was added to cell cultures (2.5 μM) at the beginning of treatment. At the end of incubation, cells were detached by trypsinization, washed in PBS, and the green fluorescence (FL1) of DHR-stained cells was analyzed using a FACSCalibur flow cytometer. The results are expressed as mean intensity of DHR fluorescence.

## 5.7. Mitochondrial depolarization assessment

The mitochondrial depolarization was assessed using DePsipher (R&D Systems), a lipophilic cation susceptible to the changes in mitochondrial membrane potential. It has the property of aggregating upon membrane polarization forming an orange-red fluorescent compound. If the potential is disturbed, the dye cannot access the transmembrane space and remains or reverts to its green monomeric form. The cells were stained with DePsipher as described by the manufacturer, and the green monomer and the red aggregates were detected by flow cytometry. The results were presented as a green/red fluorescence ratio (geomean FL1/FL2), the increase of which reflects mitochondrial depolarization.

## 5.8. Microtubule depolymerization assay

Bovine brain tubulin was isolated by the procedure described previously.<sup>38</sup> Microtubule disassembly was followed turbidimetrically as previously described,<sup>39</sup> and selected compounds (concentrations: 5, 10, 25, and 50 μM) were evaluated for the inhibition of microtubule depolymerization *in vitro*.



### 5.9. Mathematical analysis of cytotoxic interactions and IC<sub>50</sub> calculation

To analyze the type (additive, synergistic, or antagonistic) of cytotoxic interactions of different xanthenes, glioma cells were treated with different doses of each agent alone, as well as with their appropriate combinations. The cell number was assessed using a crystal violet assay and the % cytotoxicity was calculated using the following formula:  $(C - T)/C \times 100$ , where  $C$  is the cell number in control (untreated) cultures and  $T$  is the cell number in xanthone-treated cultures. The values of combination index, reflecting additive (=1), synergistic (<1), or antagonistic interactions (>1), were calculated according to the median-effect principle-based method of Chou and Talalay,<sup>40</sup> which includes the calculation of the IC<sub>50</sub> values.

### 5.10. Statistical analysis

The statistical significance of the differences was analyzed by  $t$ -test or ANOVA followed by the Student–Newman–Keuls test. The value of  $p < 0.05$  was considered significant.

### Acknowledgments

The authors acknowledge the financial support by the Ministry of Science of the Republic of Serbia (Grant Nos. 145073 and 142053).

### References and notes

- Jovanovic-Dunjic, R. In *Flore de la Republique Socialiste de Serbie V*; Josifovic, M., Ed.; Academie Serbe des Sciences et des Artes: Belgrade, 1973; pp 412–425.
- Uncini Manganelli, R. E.; Chericoni, S.; Baragatti, B. *Fitoterapia* **2000**, *71*, S95–S100.
- Baragatti, B.; Calderone, V.; Testai, L.; Martinotti, E.; Chericoni, S.; Morelli, I. *J. Ethnopharmacol.* **2002**, *79*, 369–372.
- Rivaille, P.; Massicot, J.; Guyot, M.; Plouvier, V.; Massias, M. *Phytochemistry* **1969**, *8*, 1533–1541.
- Pinto, M. M. M.; Sousa, M. E.; Nascimento, M. S. J. *Curr. Med. Chem.* **2005**, *12*, 2517–2538.
- Vieira, L. M. M.; Kijjoa, A. *Curr. Med. Chem.* **2005**, *12*, 2413–2446.
- Yoshimi, N.; Matsunaga, K.; Katayama, M.; Yamada, Y.; Kuno, T.; Qiao, Z.; Hara, A.; Yamahara, J.; Mori, H. *Cancer Lett.* **2001**, *163*, 163–170.
- Seo, E. K.; Kim, N. C.; Wani, M. C.; Wall, M. E.; Navarro, H. A.; Burgess, J. P.; Kawanishi, K.; Kardono, L. B.; Riswan, S.; Rose, W. C.; Fairchild, C. R.; Farnsworth, N. R.; Kinghorn, A. D. *J. Nat. Prod.* **2002**, *65*, 299–305.
- Laphookhieo, S.; Syers, J. K.; Kiattansakul, R.; Chant-rapromma, K. *Chem. Pharm. Bull. (Tokyo)* **2006**, *54*, 745–747.
- Ito, C.; Itoigawa, M.; Mishina, Y.; Filho, V. C.; Mukai-naka, T.; Tokuda, H.; Nishino, H.; Furukawa, H. *J. Nat. Prod.* **2002**, *65*, 267–272.
- Shadid, K. A.; Shaari, K.; Abas, F.; Israf, D. A.; Hamzah, A. S.; Syakroni, N.; Saha, K.; Lajis, N. H. *Phytochemistry* **2007**, *68*, 2537–2544.
- Pedro, M.; Cerqueira, F.; Sousa, M. E.; Nascimento, M. S.; Pinto, M. *Bioorg. Med. Chem.* **2002**, *10*, 3725–3730.
- Lee, B. W.; Lee, J. H.; Lee, S. T.; Lee, H. S.; Lee, W. S.; Jeong, T. S.; Park, K. H. *Bioorg. Med. Chem. Lett.* **2005**, *15*, 5548–5552.
- Matsumoto, K.; Akao, Y.; Ohguchi, K.; Ito, T.; Tanaka, T.; Iinuma, M.; Nozawa, Y. *Bioorg. Med. Chem.* **2005**, *13*, 6064–6069.
- Matsumoto, K.; Akao, Y.; Yi, H.; Ohguchi, K.; Ito, T.; Tanaka, T.; Kobayashi, E.; Iinuma, M.; Nozawa, Y. *Bioorg. Med. Chem.* **2004**, *12*, 5799–5806.
- Nakagawa, Y.; Iinuma, M.; Naoe, T.; Nozawa, Y.; Akao, Y. *Bioorg. Med. Chem.* **2007**, *15*, 5620–5628.
- Giese, A.; Bjerkvig, R.; Berens, M. E.; Westphal, M. *J. Clin. Oncol.* **2003**, *21*, 1624–1636.
- Loeffler, M.; Kroemer, G. *Exp. Cell Res.* **2000**, *256*, 19–26.
- Desai, A.; Mitchison, T. J. *Annu. Rev. Cell Dev. Biol.* **1997**, *13*, 83–117.
- Shi, Q.; Chen, K.; Morris-Natschke, S. L.; Lee, K. H. *Curr. Pharm. Des.* **1998**, *4*, 219–248.
- Beutler, J. A.; Hamel, E.; Vlietinck, A. J.; Haemers, A.; Rajan, P.; Roitman, J. N.; Cardellina, J. H., 2nd; Boyd, M. R. *J. Med. Chem.* **1998**, *41*, 2333–2338.
- Horwitz, S. B. *Ann. Oncol.* **1994**, *5*, S3–S6.
- Wang, T. H.; Popp, D. M.; Wang, H. S.; Saitoh, M.; Mural, J. G.; Henley, D. C.; Ichijo, H.; Wimalasena, J. J. *Biol. Chem.* **1999**, *274*, 8208–8216.
- Tan, G.; Heqing, L.; Jiangbo, C.; Ming, J.; Yanhong, M.; Xianghe, L.; Hong, S.; Li, G. *Int. J. Cancer* **2002**, *97*, 168–172.
- Zorov, D. B.; Juhaszova, M.; Sollott, S. J. *Biochim. Biophys. Acta* **2006**, *1757*, 509–517.
- André, N.; Braguer, D.; Brasseur, G.; Gonçalves, A.; Lemesle-Meunier, D.; Guise, S.; Jordan, M. A.; Briand, C. *Cancer Res.* **2000**, *60*, 5349–5353.
- Carré, M.; André, N.; Carles, G.; Borghi, H.; Brichese, L.; Briand, C.; Braguer, D. *J. Biol. Chem.* **2002**, *277*, 33664–33669.
- Costa, D.; Fernandes, E.; Santos, J. L.; Pinto, D. C.; Silva, A. M.; Lima, J. L. *Anal. Bioanal. Chem.* **2007**, *387*, 2071–2081.
- Pardo-Andreu, G. L.; Dorta, D. J.; Delgado, R.; Cavalheiro, R. A.; Santos, A. C.; Vercesi, A. E.; Curti, C. *Chem. Biol. Interact.* **2006**, *159*, 141–148.
- Pardo-Andreu, G. L.; Delgado, R.; Velho, J. A.; Curti, C.; Vercesi, A. E. *Arch. Biochem. Biophys.* **2005**, *439*, 184–193.
- Hostettmann, K.; Tabacchi, R.; Jacot-Guillarmod, A. *Helv. Chim. Acta* **1974**, *57*, 294–301.
- Goetz, M.; Manillio, F.; Jacot-Guillarmod, A. *Helv. Chim. Acta* **1978**, *61*, 1549–1554.
- Sakamoto, I.; Tanaka, T.; Tanaka, O.; Tomimori, T. *Chem. Pharm. Bull.* **1982**, *30*, 4088–4091.
- Jankovic, T.; Krstic, D.; Aljancic, I.; Savikin-Fodulovic, K.; Menkovic, N.; Vajs, V.; Milosavljevic, S. *Biochem. Syst. Ecol.* **2005**, *33*, 729–735.
- Trajkovic, V.; Badovinac, V.; Popadic, D.; Hadzic, O.; Stojkovic, M. M. *Immunology* **1997**, *92*, 402–406.
- Kaludjerovic, G. N.; Miljkovic, D.; Momcilovic, M.; Djinic, V. M.; Mostarica Stojkovic, M.; Sabo, T. J.; Trajkovic, V. *Int. J. Cancer* **2005**, *116*, 479–486.
- Mijatovic, S.; Maksimovic-Ivanic, D.; Radovic, J.; Miljkovic, D.; Harhaji, L.; Vuckovic, O.; Stosic-Grujicic, S.; Mostarica Stojkovic, M.; Trajkovic, V. *Cell. Mol. Life Sci.* **2005**, *62*, 589–598.
- Shelanski, M. L.; Gaskin, F.; Cantor, C. R. *Proc. Natl. Acad. Sci. U.S.A.* **1973**, *70*, 765–768.
- Gaskin, F.; Cantor, C. R.; Shelanski, M. L. *J. Mol. Biol.* **1974**, *89*, 737–755.
- Chou, T. C.; Talalay, P. *Adv. Enzyme Regul.* **1984**, *22*, 27–55.